Demonstration of radial trace domain filtering on the Shaganappi 1998 2-D geotechnical survey

David C. Henley

ABSTRACT

In a companion chapter, we introduced and demonstrated the use of the radial trace (R-T) transform in an effective technique for attenuation of coherent noise. We describe here the step-by-step repetitive use of the technique, as embodied in a set of ProMAX functions, on a data set which has proven difficult to image because of the extremely high level of source-generated noise on the shot records. In the end, we achieve an image consistent with the known geologic setting in which the survey was performed. Since minimal processing, other than coherent noise attenuation, was applied to these data, the improvement in imaging is attributable mostly to the noise reduction achieved.

The purpose of this demonstration is twofold: to show the versatility and utility of radial trace (R-T) methods in diagnosing and attenuating coherent noise; and to advocate a more hands-on analytic approach to data processing problems such as coherent noise attenuation. By addressing each noise mode separately in an iterative approach, we acquire a much better feel for the data and the relative strength of the modes than we do with an all-or-nothing approach like F-K filtering.

INTRODUCTION

The radial trace transform and its characteristics have been described in an accompanying chapter in this report, in which we introduced the use of simple filtering techniques in the R-T domain to effectively attenuate coherent noise while preserving lateral variations in the input X-T trace panel, such as static shifts (Henley, 1999, 1). In that material, we presented noise attenuation both on real data from the Blackfoot 2-D experiment, and, in comparison with F-K methods, on a simple synthetic shot gather. The results of noise reduction on the Blackfoot data were shown to influence the interpretability of the final section. For moderately noisy data like those at Blackfoot, however, other techniques can also be successfully used to obtain interpretable results. In the present work, we demonstrate the use of R-T filter techniques on data that have such a small signal to noise ratio that other image improvement methods, like F-X deconvolution and trace mixing, have had only limited success.

The acquisition and early processing of the 1998 Shaganappi geotechnical data are described in the 1998 CREWES research report (Bland et al., 1998), and details may be found there. For our demonstration, we selected the 700 metre long 2-D line acquired using a Bison EWG-II accelerated weight drop (thumper) as seismic source and a moving 40 station receiver spread, with receivers 5 metres apart. The results we present here are not intended for comparison with earlier results, but are intended to serve as a step-by-step illustration of how systems of coherent noise (various wave modes) can be systematically removed one at a time using the R-T filtering and

diagnostic techniques we have developed. As in the Blackfoot example, we use only the most rudimentary processing on the Shaganappi data, other than the R-T domain techniques we applied, so that observed effects are due mainly to the R-T filtering. The algorithms we describe are embodied in ProMAX operations which are more fully described in another chapter in this report (Henley, 1999, 2).

METHOD

A trend has emerged in seismic processing in recent years in which human interaction with the data is minimized in favor of automatic or canned process flows, in order to handle the increasingly large sets of digital data that comprise modern seismic surveys. Optimization of processes and parameters for problem data sets requires repeated, detailed examination of the data at various stages of processing, however. Nevertheless, often only cursory screening for quality control of acquisition geometry and display parameters precedes submission of difficult data to a canned process flow. Our intention with the introduction of R-T filter methods is to reverse that trend, since repeated examination of the basic data after application of various processing options forms a major part of the technique. As implied by the characteristics of the R-T transform described in the introductory chapter (Henley, 1999, pro1), examination of trace gathers and stacks and their R-T transforms is an essential and intuitive part of designing filters in this domain. Hence, in the following, we describe every analysis step as a guide for prospective R-T processors.

We have software available for both R-T analysis and R-T filtering of X-T panels, and we use both in our processing. There are two "styles" of radial trace transform. In the R-T fan transform the radial trace origin is near a "source" position on the X-T trace panel, and the radial traces span a wide range of apparent velocity when sampling the X-T domain. For the R-T dip transform, on the other hand, the radial trace origin is far from the X-T panel, and the radial traces have only a narrow range of apparent velocities to align them with events of constant dip on the X-T panel. In our analysis, we often examine an X-T panel first using a fan transform, then a dip transform, to see which appears to isolate a particular linear noise best in the R-T domain. Application of a filter to the R-T traces, followed by a re-display, *still in the R-T domain*, can assist in choosing the best type of R-T domain filter to apply to the X-T data. After examination of the raw X-T panel, its R-T transform, and the filtered R-T transform, we then apply the full R-T filter algorithm (R-T transform-filter-inverse R-T transform) to the raw X-T panel and compare the filtered X-T panel with the raw version. This sequence of steps occurs at each stage of coherent noise removal described below.

Measuring apparent velocity of noise on an X-T panel as well as estimating the position of its origin provides guidelines for setting R-T transform parameters. The R-T trace display, on the other hand, can provide confirmation of R-T transform parameter choice as well as assistance in adjusting those parameters. For example, a near-vertical linear noise inclined *towards* the R-T transform origin indicates that the origin time coordinate parameter should be *increased* to make the event more vertical, while an event inclined *away* from the origin indicates a required *decrease* in the time coordinate. Because the R-T transform normally contains many times more

traces than the X-T panel, we usually display the X-T panel as variable-area/wiggle traces and the R-T panel as variable-density.

The raw data

We have described the coherent noise problem on the Shaganappi data as severe. Figure 1 shows four shot gathers from the line as an illustration of the magnitude of the problem. At least three separate wave modes can be seen to dominate these records, and unfortunately, none of these are reflections. To show that simple CDP stacking and bandpass filtering are insufficient to handle the noise, figure 2 is the CDP stack of this line after initial muting and a 20-125 Hz bandpass applied in the X-T domain to the shot gathers. The dominance of the coherent noise in this section is obvious; and in fact, what appear to be relatively strong reflections in the right half of the shallow section are simply the stacked high-velocity near-surface coherent noise whose apparent velocity is nearly equal to the hyperbolic moveout for reflections over the very short offset range (0-200 metres) of these data. While a few legitimate reflections are visible in the 100-200 ms range to the left of centre, this section could never be considered a usable image.

In what follows, we refer to linear dipping events as having an apparent velocity, meaning that we define their dip in terms of metres of lateral offset per second of travel time. We use the convention that events dipping down in the direction of decreasing signed offset have negative velocity, and those dipping down toward increasing offsets have positive velocity. In this convention, a vertical event has zero velocity and a horizontal one, infinite velocity. If we refer to an event or R-T dip filter with a +/- velocity designation, we mean that both positive and negative velocity events are present or dip filters of both positive and negative velocities have been applied.

A logical approach to filtering these data is to start with the strongest noise first, which in this case is the air-blast. We find it instructive to examine an R-T fan transform of the data as a general diagnostic, in conjunction with the input shot gather itself. Accordingly, in figure 3 are the radial fan transforms of two of the shot gathers in figure 1. Without additional information, we have placed the origin of the transform at the apparent shot origin for this diagnostic. The air-blast is seen in figure 3 to be oriented near-vertical, but with some horizontal “striping”. The striping is evidence of the spatial aliasing of the air-blast at some frequencies, even for the relatively fine 5 metre geophone spacing used on this line. Nevertheless, the underlying low frequencies can be suppressed by a low-cut filter in the R-T domain. The other prominent noise on these R-T transforms is the near-surface coherent noise, which appears here as relatively low-frequency linear events inclined toward the origin. To test how well these two noise modes can be attenuated in the R-T domain, we present in figure 4 the results of filtering the transforms in figure 3 with a 20-125 Hz bandpass. It can be seen that not only has the air-blast been significantly reduced, but the low-frequency components of the high-velocity near-surface modes are attenuated as well.

An alternative to the R-T fan transform is the R-T dip transform, in which we specify only a nominal apparent velocity and a tolerance around that value. These two

parameters define a narrow fan of R-T traces whose velocities are centred on the nominal velocity and whose velocity range is defined by the tolerance parameter. Since the air-blast and its multiples have a well-defined velocity around 300 m/sec, and, in the case of the multiples, more than one apparent origin, we surmise that a dip transform might be more suitable in isolating this noise. Figure 5 is the dip transform centred at 300 m/sec of two of the shot gathers in figure 1. In addition to the overall difference in shape of this transform, we note that the air-blast event and its multiples are more nearly linear here, as well as more near vertically aligned and less severely spatially aliased. Application of the same 20-125 Hz bandpass to this transform results in figure 6, in which we can see that the air-blast and multiples are attenuated more severely than in figure 4. These observations lead us to choose an R-T domain dip filter rather than a fan filter for removal of this noise. Because the noise is so strong compared to other events present, we chose to apply an AGC operator in the R-T domain, as well, to additionally attenuate the R-T traces on which this noise is isolated. The results of applying the R-T domain dip filter at 300 m/sec, as well as a similar filter at –300 m/sec (to deal with the negative velocity scattered modes) to the shot gathers of figure 1 is shown in figure 7. The improvement over figure 1 is obvious. Portions of reflections can now be seen throughout much of the data. Some air-blast can still be seen due to the alignment of spatially aliased frequency components not attenuated by the R-T filter.

Filter pass number two

Figure 7 also shows that the strongest remaining coherent noise mode is the higher frequency components of the shallow high velocity arrivals. Since these appear to have no particular common origin, we elect to examine them with an R-T dip transform centred at a velocity of 1900 m/s, which we measure on the shot gathers in figure 7. Figure 8 is the R-T dip transform of two of the figure 7 gathers, centred at 1900 m/sec. The high velocity mode is seen to be vertically oriented and unaliased in this transform, so application of the 20-125 Hz bandpass results, in figure 9, in near complete removal of this mode. Reflections can now be seen on these R-T transforms, crossing the data panels almost at right angles to the long axes. Figure 10 shows the X-T gathers of figure 7 after R-T domain dip filter passes at +/- 1900 m/sec, the negative velocity pass again intended to remove negative velocity scattered energy. As on the R-T transform displays, reflections are now the dominant events. Linear noise is still obvious on these records, however, so we continue, even though these data are beginning to look a bit mixed. The high-velocity dip filters are the largest contributors to this, since their velocity is so close to that of the reflection events that the filter response functions smear the data somewhat in *near*-horizontal directions.

Filter pass number three

At this point we could choose either a dip transform or a fan transform to further analyze the data. We elect to try the fan transform (figure 11). Although we see that the predominant energy in this display is near-horizontal reflected energy, some near-vertical linear modes are clearly still present. Application of the 20-125 Hz bandpass results in figure 12, on which yet more linear noise becomes visible in the right-dipping events on these transforms. Figure 13 displays the result of applying the

comparable R-T fan filter to the shot records of figure 10. Once again, the records have been improved. However, at least one mode of linear noise remains.

Filter pass number four

Because the remaining noise on figure 13, at +/- 950 m/sec has half the velocity of the previously filtered +/- 1900 m/s events, we assume that the noise is likely due to energy spatially aliased from that higher-velocity mode. Nevertheless, we treat it as an independent mode by transforming it with an R-T dip transform centred at 950 m/sec, the results of which appear in figure 14. The near-vertical stripes again indicate a susceptibility to filtering in this domain, as the 20-125 Hz bandpass in figure 15 confirms. The X-T domain result of filtering the shots in figure 13 with an R-T domain dip filter at +/- 950 m/sec is shown in figure 16. These records show little evidence of any remaining linear noise. While the *appearance* of the reflections on these records seems more mixed than those in figure 13, much of the increased smoothness is actually attributable to the removal of lateral amplitude variations caused by interference with the +/- 950 m/sec noise.

Stack number two

Figure 17 shows the CDP stack of all shots on the line after the previously described passes of R-T domain filtering. We analyzed reflection moveout on shot gathers to build a simple NMO velocity function for these data, and the same function was applied for NMO correction for both the brute stack in figure 2 and the R-T filtered stack in figure 17. Since there is no evidence of significant statics on these compressional mode data, we ignored static corrections for all stacks, and applied only a simple and very minimal initial mute function to the shot gathers. The improvement of the stack in figure 17 with respect to the brute stack in figure 2 is evident. Close examination of the section shows a minor amount of linear noise remaining. Not surprisingly, its velocity is about +/- 475 m/sec, which indicates another alias of the original +/- 1900 m/s mode.

Post-stack filter pass

Since we intended to perform a mild post-stack deconvolution on this line, we decided to remove the remaining linear noise by application of a post-stack R-T dip filter. The results of this are shown in figure 18, and a mild post-stack predictive deconvolution results in figure 19, in which we broaden the signal bandwidth slightly. Particularly in the shallow part of this section, we see many events that have the appearance of diffractions extending over many traces laterally. Migration of these data is indicated!

Post-stack migration

Migration is an imaging process closely coupled to interpretation, and is usually an iterative process involving many iterations and modifications of velocities. Furthermore, it is most accurately a 3-D pre-stack process; and 2-D post-stack approximation often leads to image distortion. Nevertheless, after experimenting with a wide range of migration velocities, apertures, and dip limits, we applied 2-D post-stack migration to the data. Figure 20 reveals one version, not necessarily the best), of

Kirchhoff post-stack migration applied to the section of figure 19. We make no attempt at interpretation here other than to comment that the image is consistent with the location of the seismic line at an oblique angle across river terrace deposits of relatively recent origin, containing known clay and gravel lenses, abandoned channels, and so forth, overlying deeper, more uniformly deposited sediments.

DISCUSSION

This exercise is an admittedly heavy-handed use of R-T domain filtering for demonstrating its potential for improving imaging. The point is to show an intuitive, hands-on, step-by-step approach to coherent noise removal. In all likelihood, an F-K filter could be designed to accomplish at least some of the noise removal achieved here, but probably at increased cost in lateral trace amplitude smearing. The process shown here involves diagnosis and assessment at every new stage of noise removal, and we could omit any particular stage at our discretion, whereas F-K filtering provides less opportunity to be selective. It tends to be an all-or-nothing approach.

Our demonstration of filtering the Shaganappi data involved seven separate pre-stack R-T filter passes and two post-stack R-T dip filters applied for both positive and negative velocities. Application of so many bandpass filters of the same bandwidth might be of concern because of the implied steepness of the composite filter cutoff slopes. If this is a concern, the slopes of the individual filters are within the control of the processor and can be made milder, when multiple R-T passes are to be employed.

Apparent phase change of events due to R-T filtering has been identified as a possible concern to interpreters. The phase of the filter implemented in the ProMAX R-T filter module is zero. Repeated application of a zero-phase filter to data whose phase is other than zero *will* result in phase change, but repeated R-T filter passes are needed usually only on the very noisiest data, in which event *phase* is of much less concern than simple event *visibility*.

As mentioned earlier, the R-T dip filter passes at +/- 1900 m/sec appear to cause some lateral event smearing because of the proximity of the apparent dip velocity to the reflection moveout velocity on these data. If there were significant statics on these data, we would likely have attempted to pick and derive residual statics *prior* to applying the +/- 1900 m/sec dip filters, although the records in figure 7 do not appear to have high enough signal/noise ratio to successfully correlate reflection events.

CONCLUSIONS

We conclude from this exercise that R-T domain filtering techniques offer a useful, systematic and instructive way to identify and remove coherent noise on severely noisy data. Because it is a hands-on approach, the processor has much more control over the results, as well as a better intuitive feel for the data, than if a more conventional technique were used. Although we did not process these data in this fashion, a process flow *can* be set up in the ProMAX environment so that screen displays of each shot gather at each stage of filtering can be viewed during the process of building the stack. The author has done this on other data and can attest to

the intimate knowledge acquired of a particular data set in the course of several iterations of this process.

ACKNOWLEDGEMENTS

The author thanks the CREWES staff and sponsors for support of this project, and thanks the staff for much useful discussion on these results (especially Pat Daley and John Bancroft). The permission of Shell Canada Ltd. and the Shell Group to use and expand these techniques, begun while the author was an employee, is gratefully acknowledged.

REFERENCES

Bland, H., Stewart, R.R., Lu, H., Cordsen, A., and Werner, M., The Shaganappi geotechnical experiments: 2-D and 3-D multicomponent seismic surveys and geologic logs, CREWES Research Report **10**, Ch 34.

Henley, D.C., Coherent noise attenuation in the radial trace domain: introduction and demonstration, CREWES Research Report **11**.

Henley, D.C., Radial trace computational algorithms at CREWES, CREWES Research Report **11**.

FIGURES

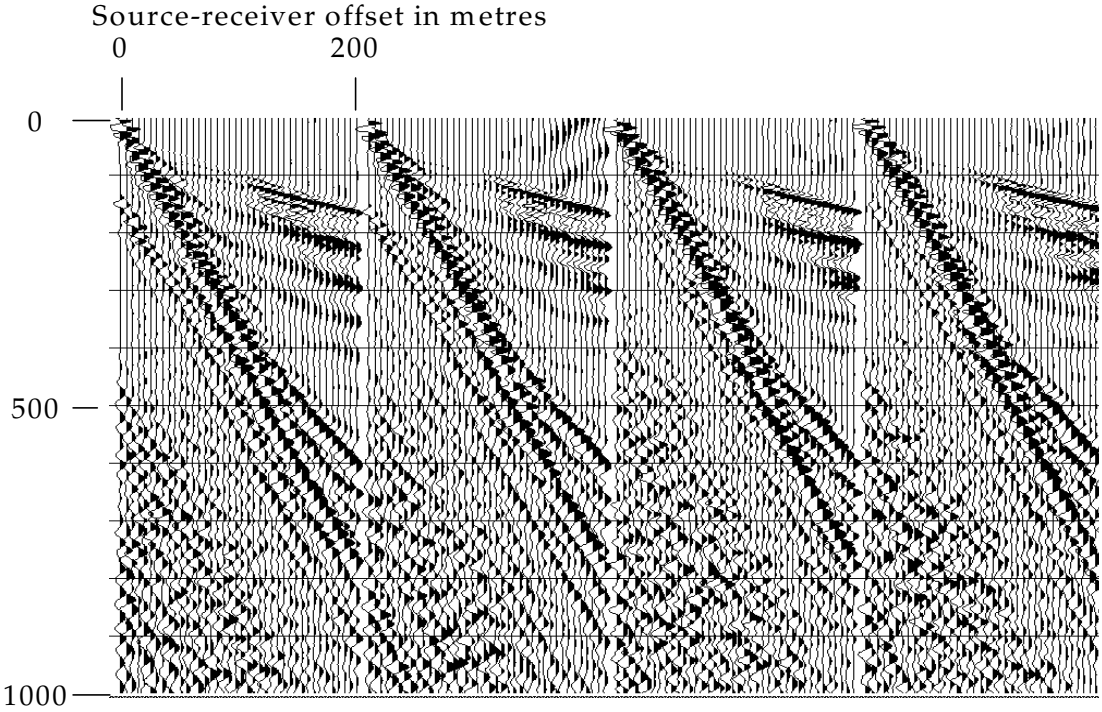

Figure 1 – Raw shot gathers from the 2-D Shaganappi geotechnical survey. These shots are compressional wave data acquired with the thumper source.

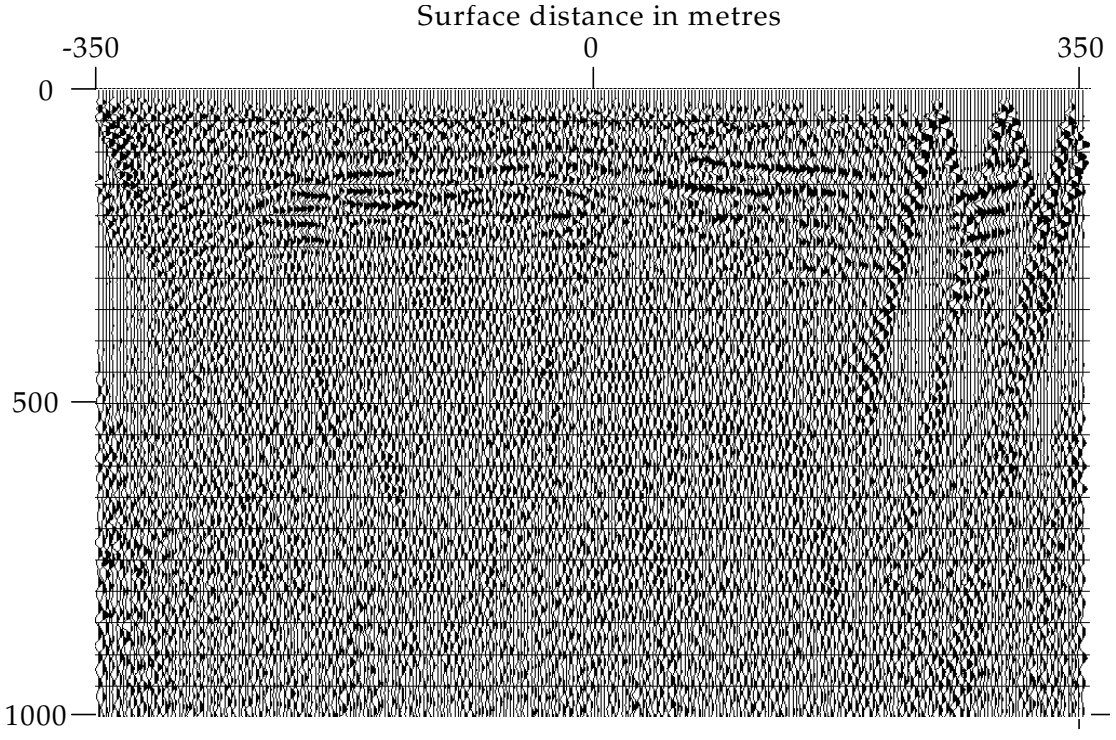

Figure 2 – Brute stack of Shaganappi 2-D thumper line with 20-125 Hz filter applied to input shot gathers.

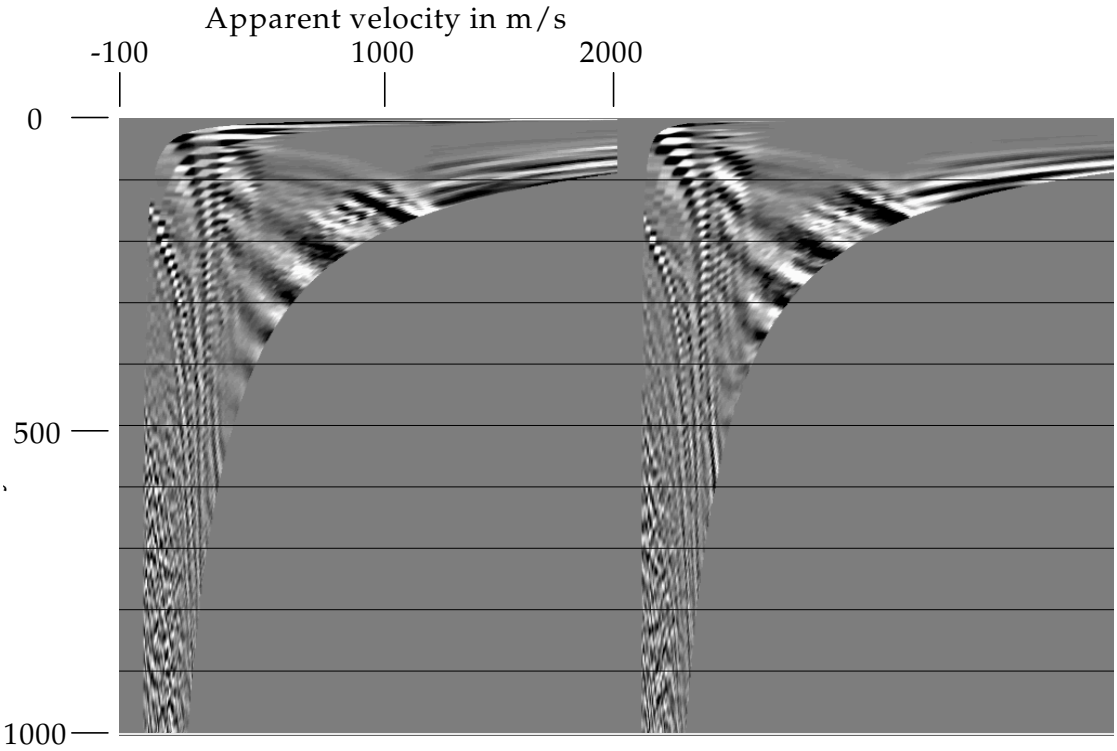

Figure 3 – R-T fan transforms of two shot gathers from figure 1. Air-blast event is near-vertical, but shows spatial aliasing (horizontal banding).

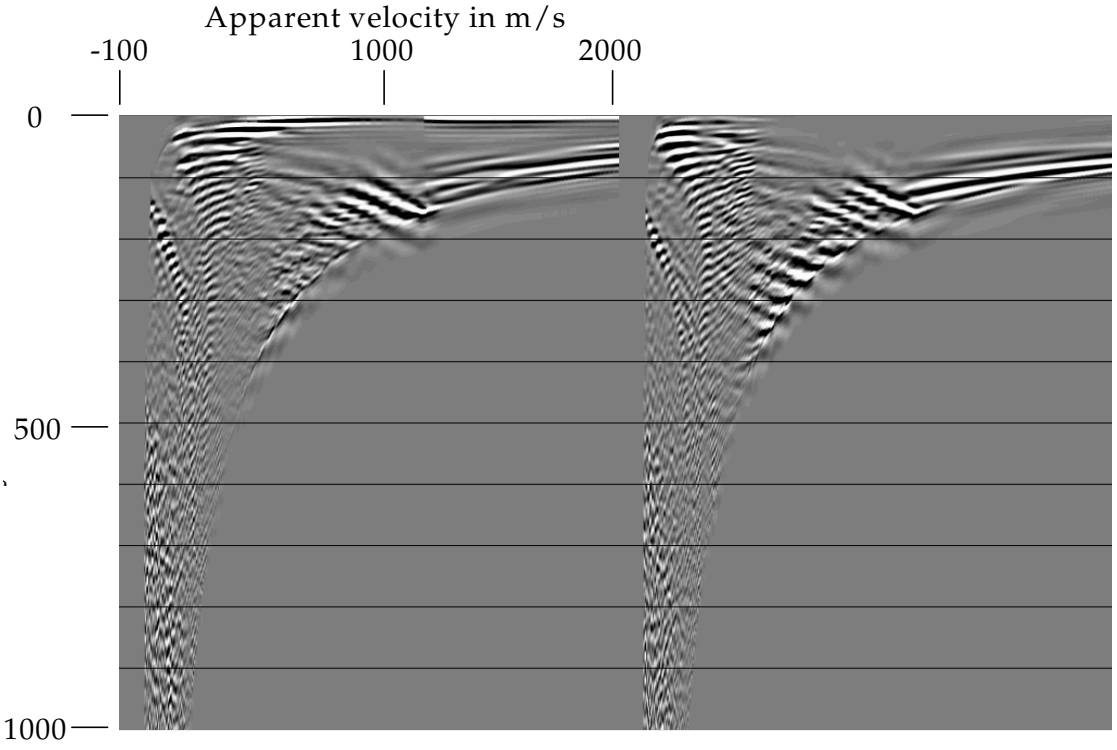

Figure 4 – R-T fan transforms of figure 3 filtered with 20-125 Hz bandpass. Low-frequency part of air-blast is attenuated, but not aliased part.

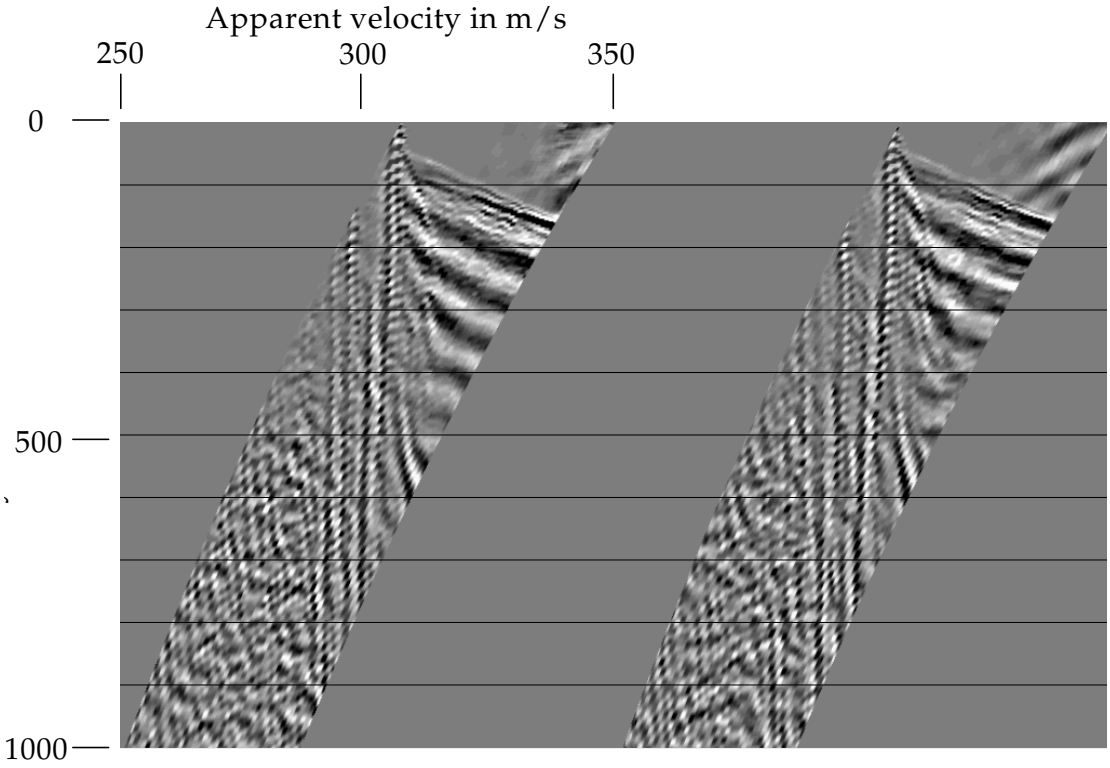

Figure 5 – R-T dip transform of two shot gathers from figure 1. Air-blast is more nearly vertical in this domain, less spatially aliased.

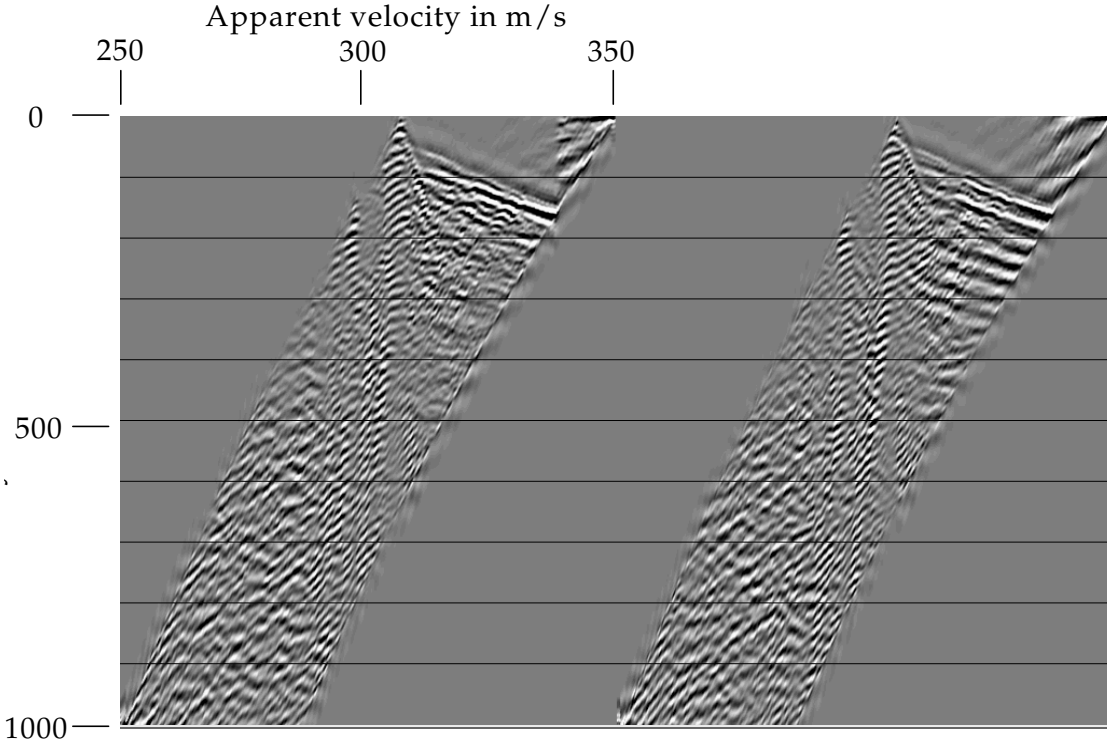

Figure 6 – R-T dip transform after 20-125 Hz bandpass filter. Air-blast more completely removed in this domain, with less surviving aliased energy than for fan transform.

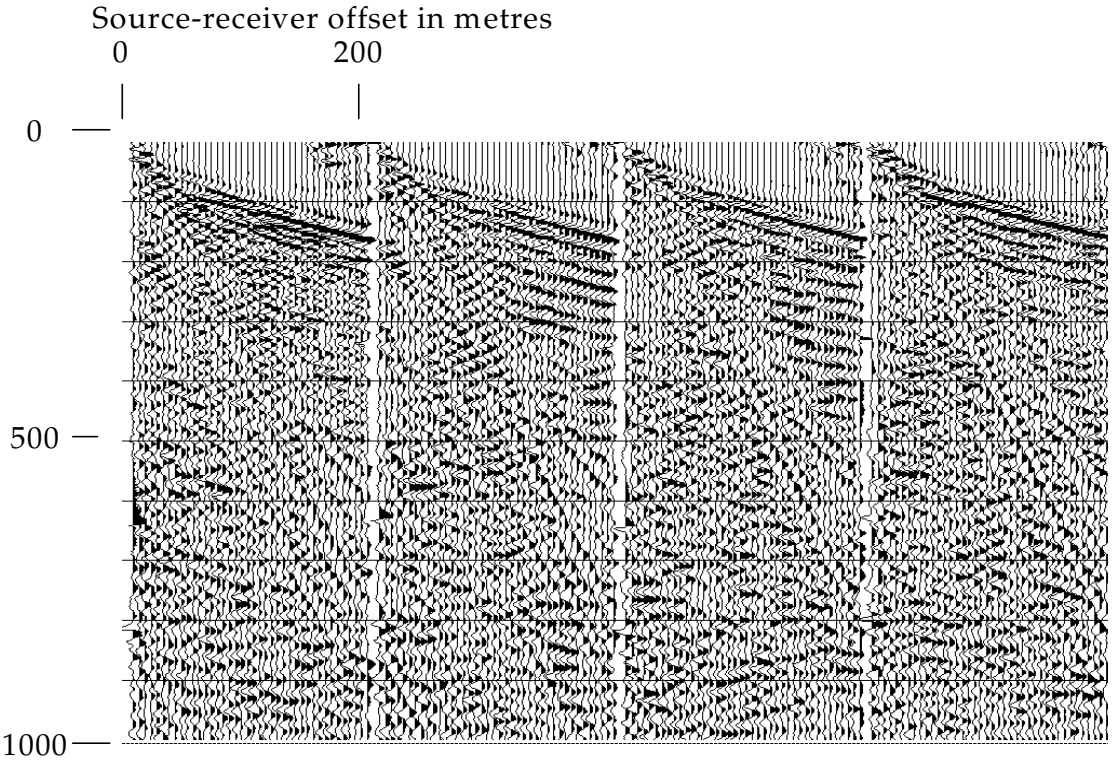

Figure 7 – Shot gathers of figure 1 after application of R-T domain dip filters at +/- 300 m/sec. Some reflection energy can now be seen.

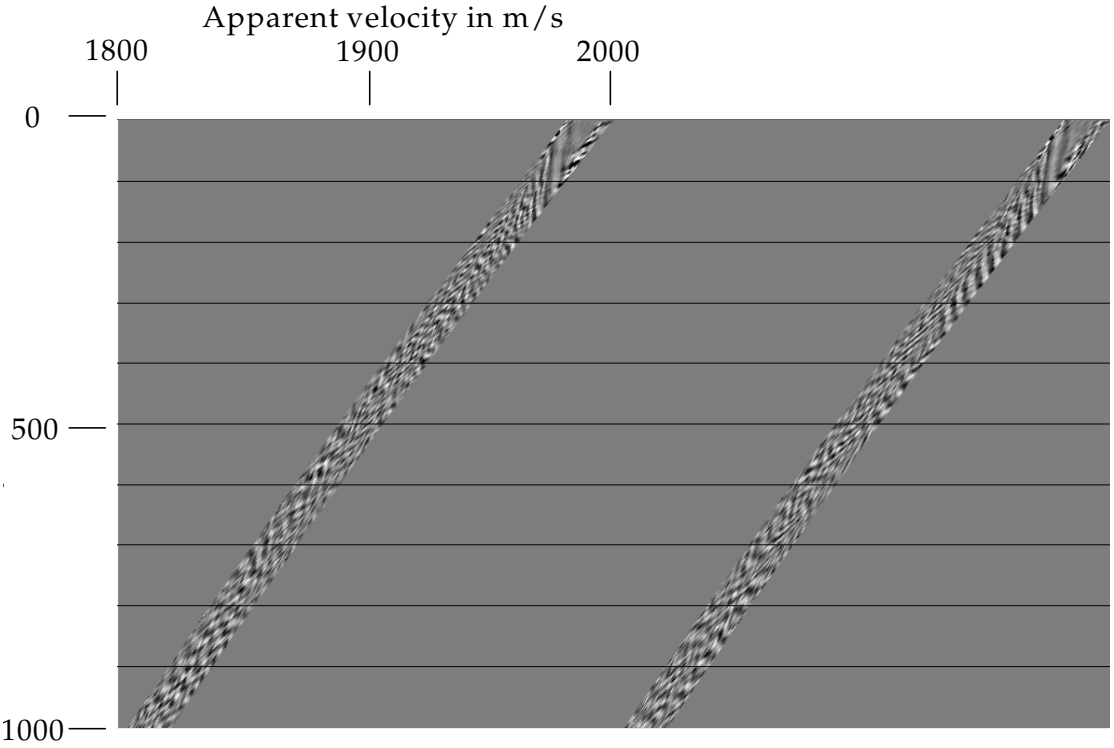

Figure 8 – R-T dip transforms of two gathers from figure 7, centred at 1900 m/sec. Parallel, near-vertical bands are shallow waveguide mode events.

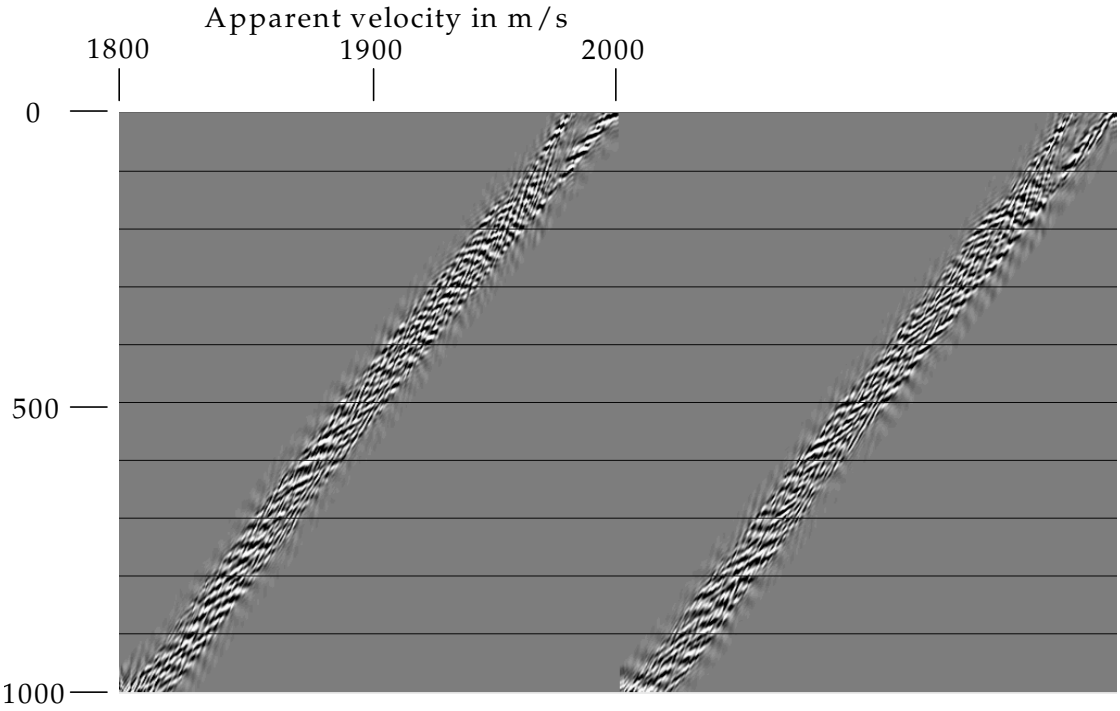

Figure 9 – R-T dip transform of shot records in figure 7 after 20-125 Hz bandpass filter. Reflections are now prominent on these transforms.

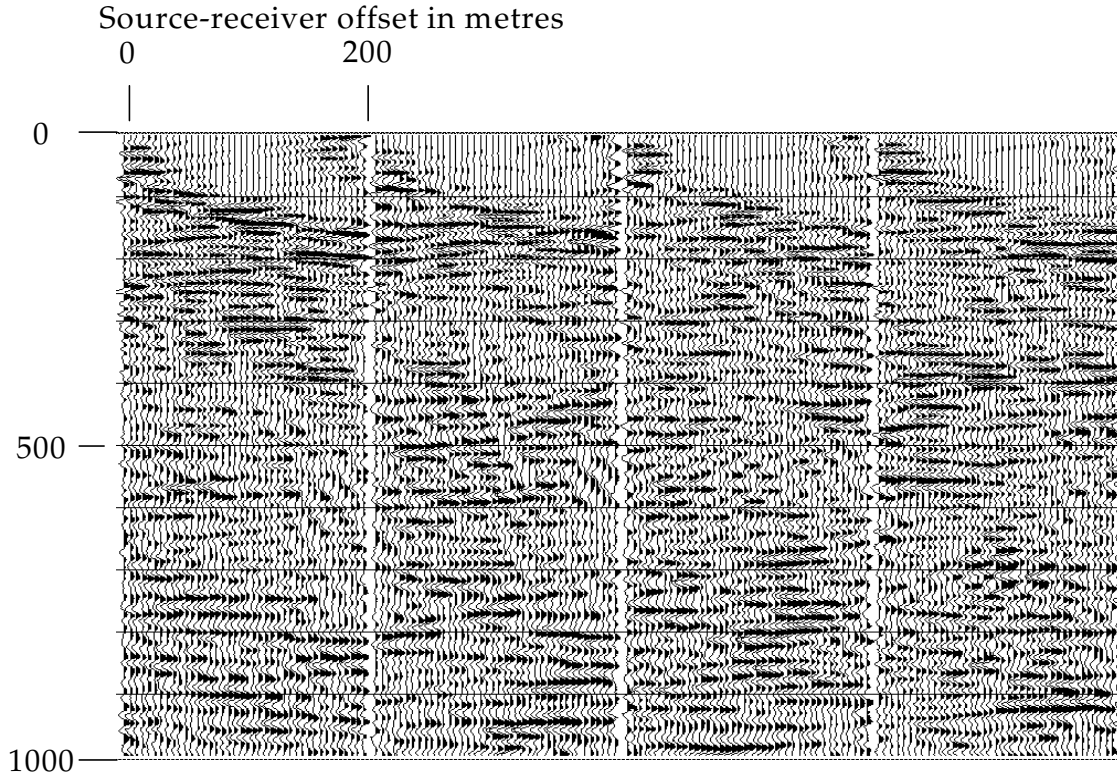

Figure 10 – shot gathers from figure 7 after R-T dip filters of +/- 1900 m/sec. Reflections are now very apparent. More linear noise now apparent.

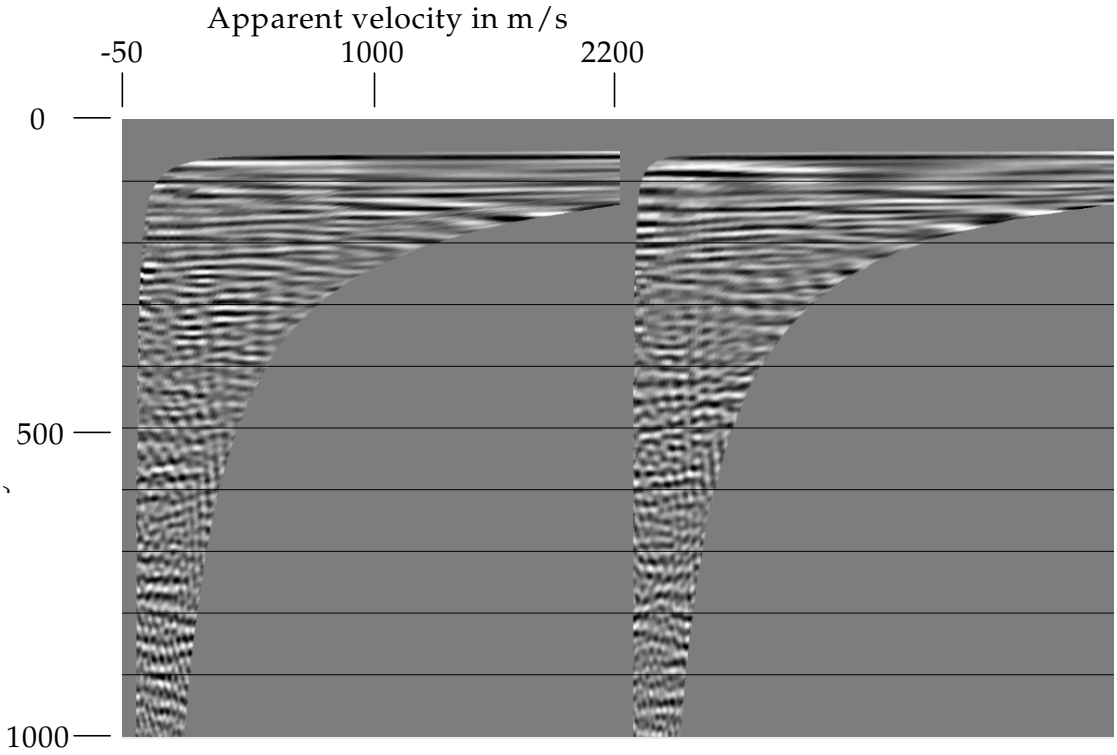

Figure 11 – R-T fan transforms of two shots from figure 10. Most energy is near-horizontal reflection energy, but some near-vertical coherent noise stripes still evident.

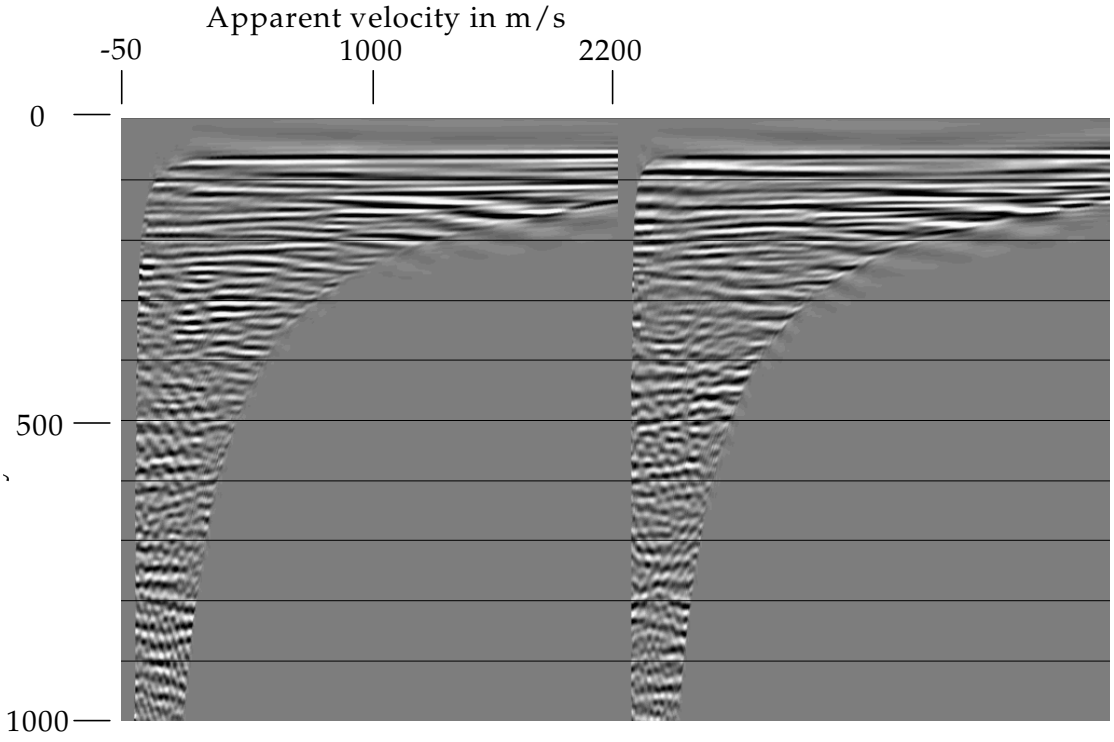

Figure 12 – R-T fan transforms of figure 10 shots after 20-125 Hz bandpass. Near-vertical events are gone, but right-dipping events indicate presence of still more coherent noise!

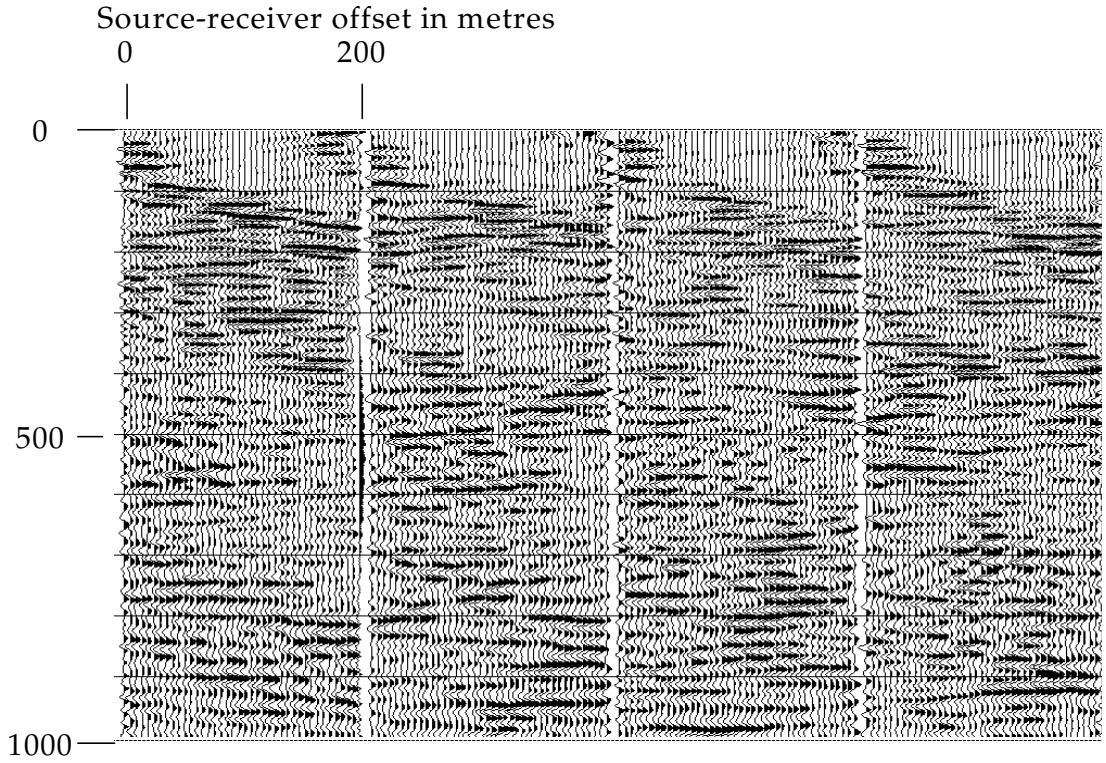

Figure 13 – shots of figure 10 after application of R-T fan filter. At least one mode of coherent noise remains on these gathers.

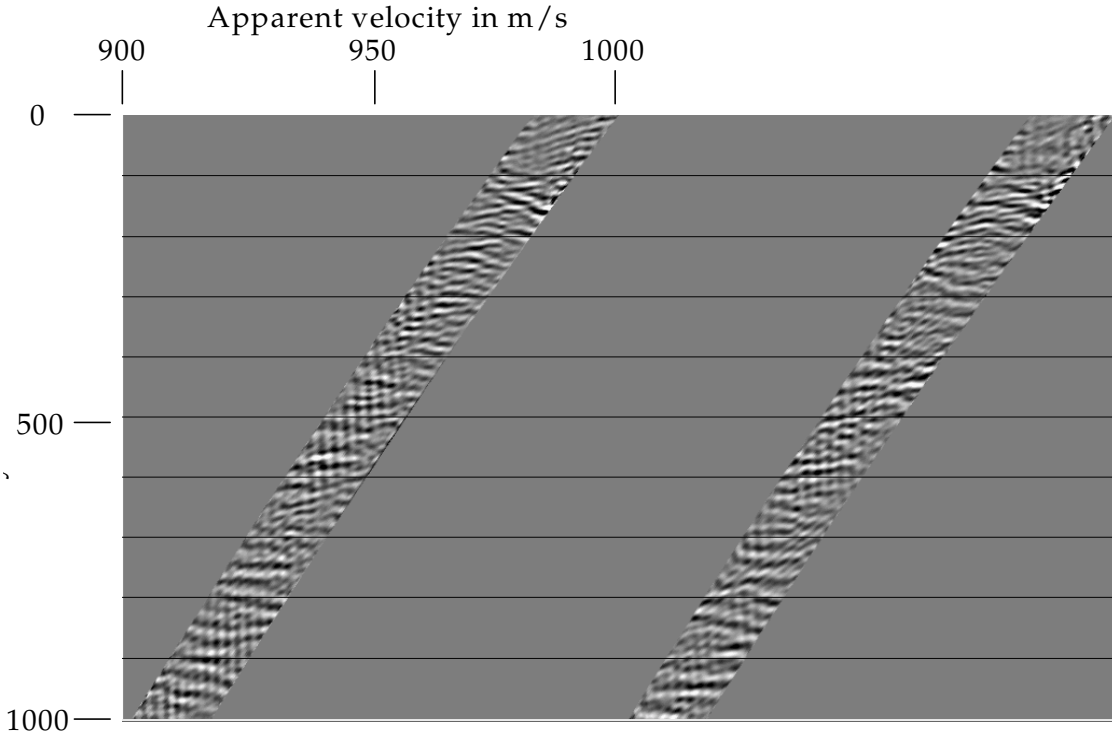

Figure 14 – R-T dip transforms of two shots from figure 13, centred at 950 m/sec. Near-vertical stripes indicate coherent noise vulnerable to low-cut filter.

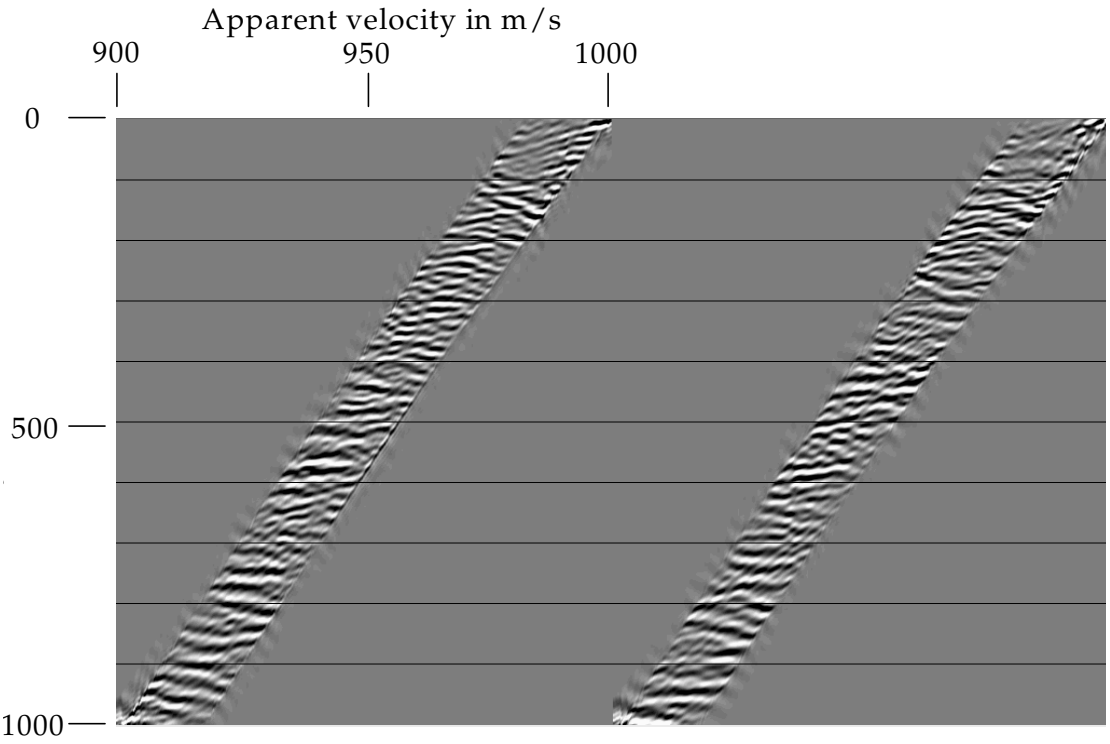

Figure 15 – R-T dip transforms of shots from figure 13 after 20-125 Hz bandpass filter. Virtually all remaining energy is near-horizontal, reflection-like energy.

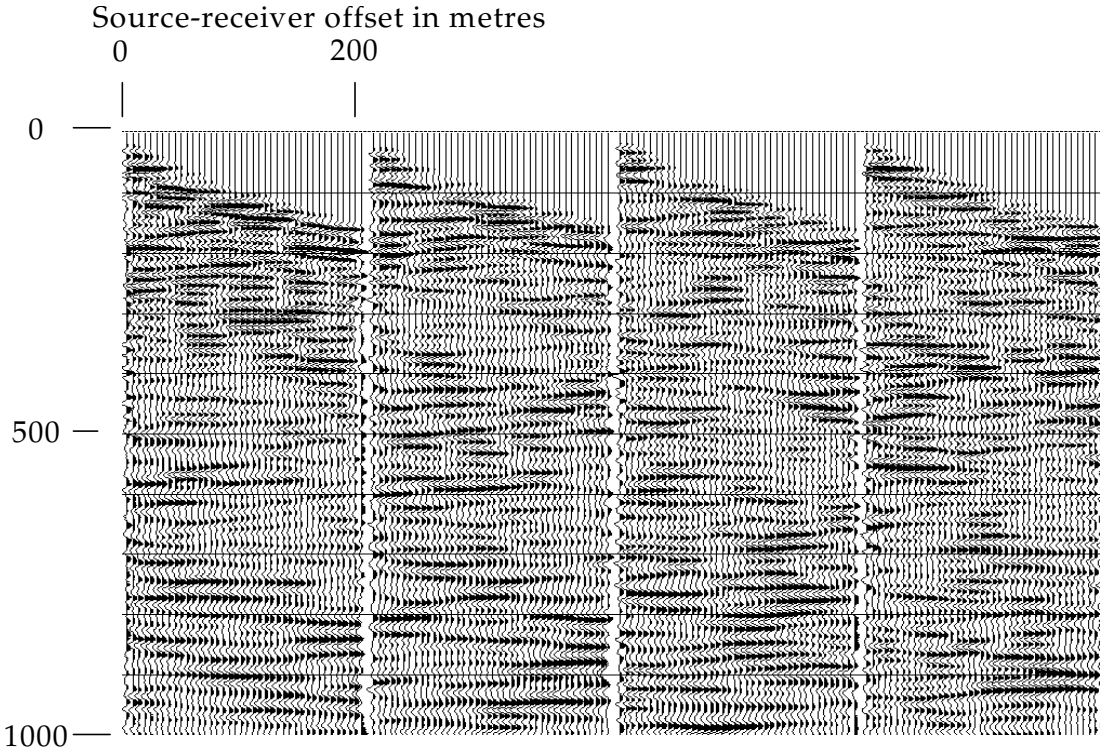

Figure 16 – shots from figure 13 after R-T dip filters at +/- 950 m/sec. Any residual coherent noise is very low in amplitude.

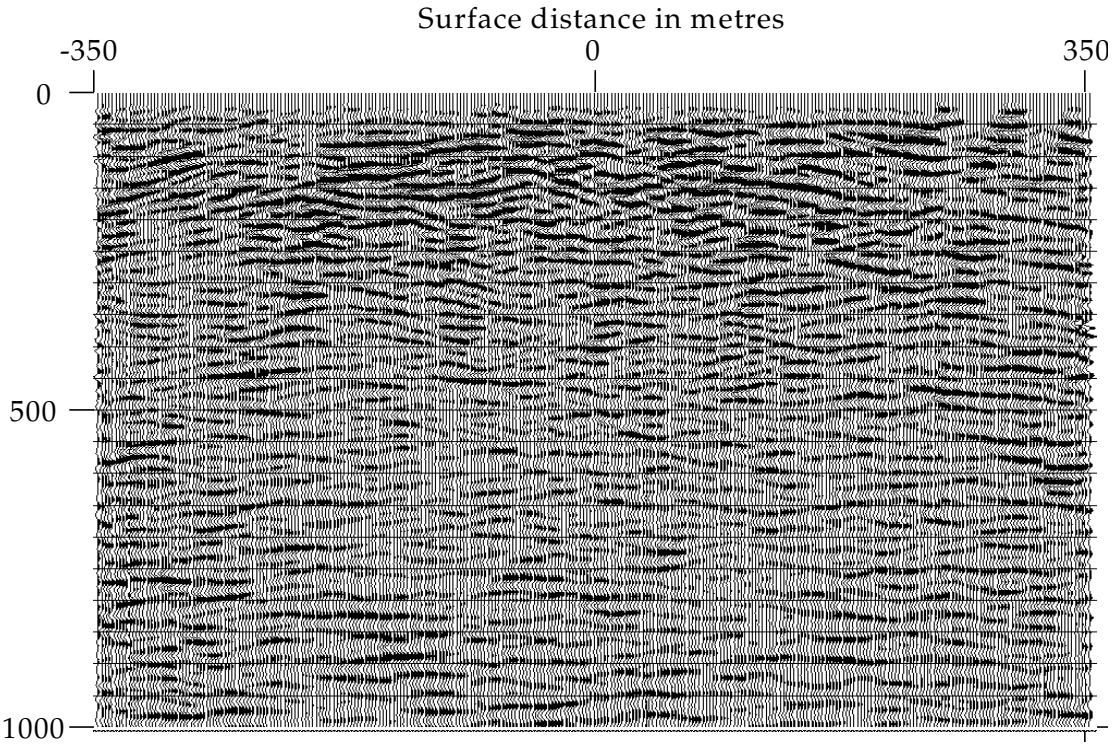

Figure 17 – CDP stack of Shaganappi line after application of R-T filter passes to shot gathers. Residual coherent noise barely visible at +/- 475 m/sec.

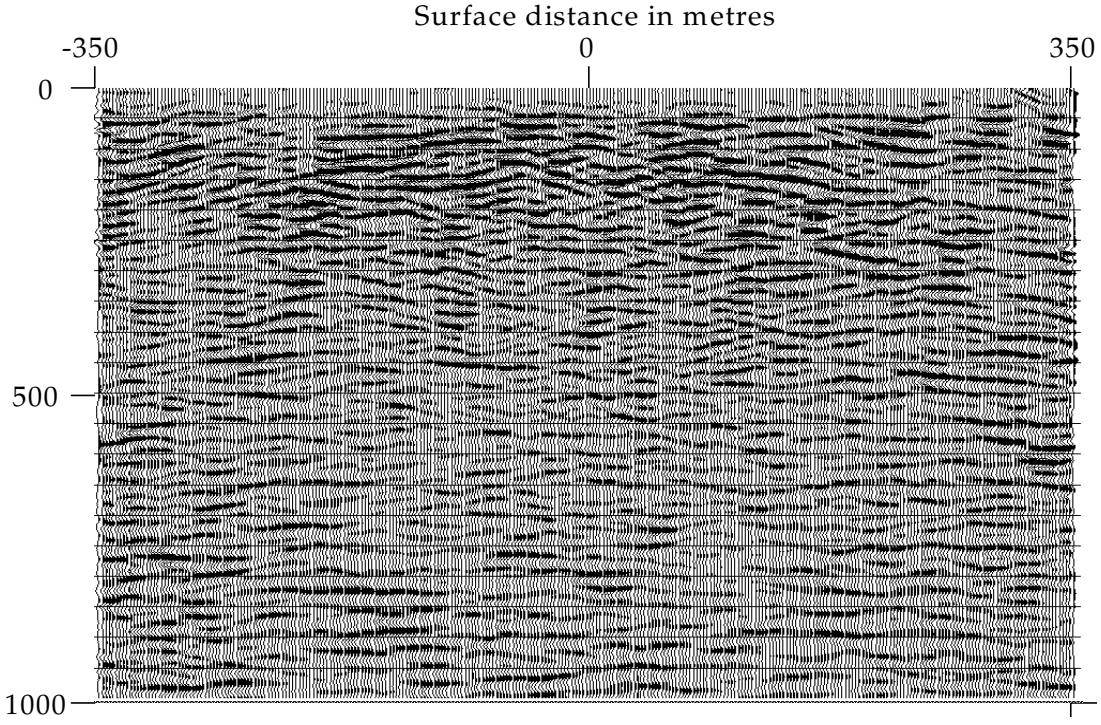

Figure 18 – section of figure 17 after post-stack application of R-T dip filters at +/- 475 m/sec.

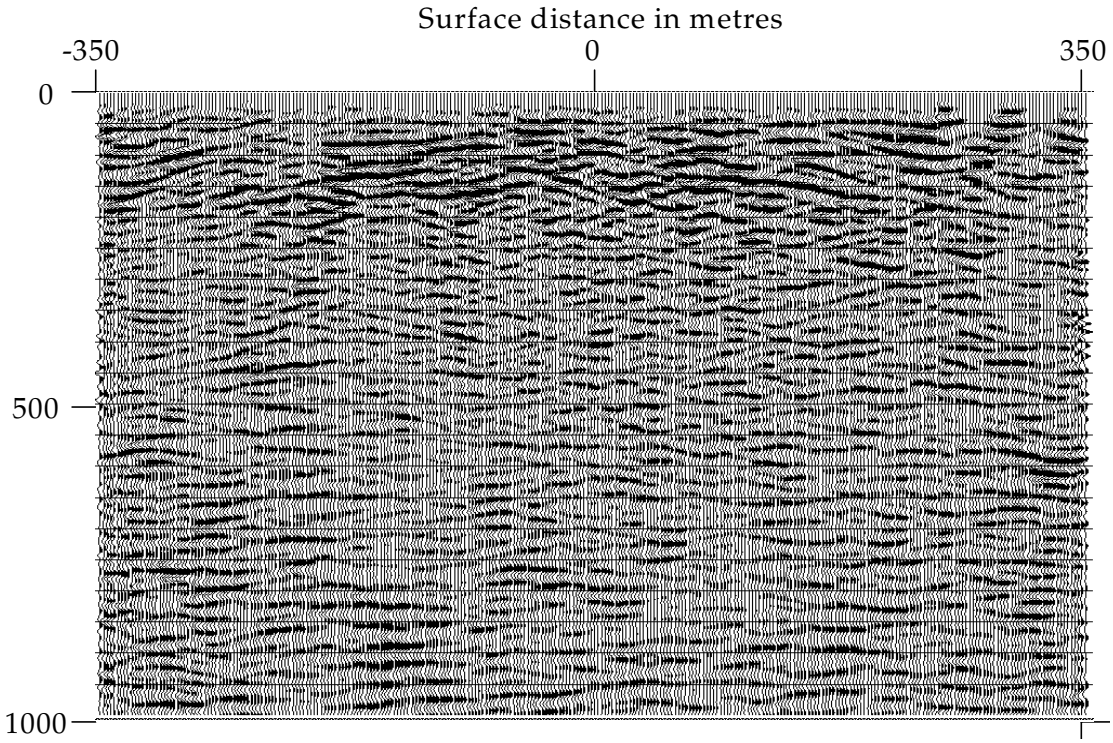

Figure 19 – Section of figure 18 after mild post-stack predictive deconvolution. Many diffraction-like events evident in the shallow part of this section.

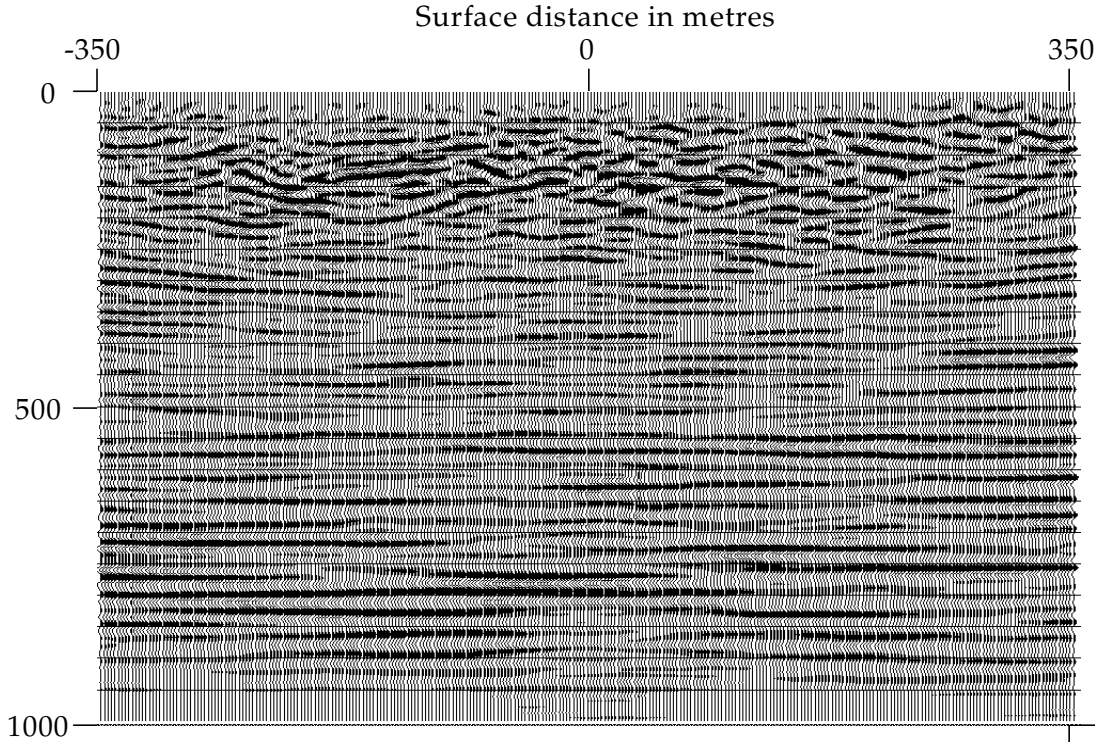

Figure 20 – Section of figure 19 after post-stack Kirchhoff time migration. This image is consistent with the known geology of the region.